

## Titanium Dioxide Nanotubes in Chloride Based Electrolyte: An Alternative to Fluoride Based Electrolyte

(Nanotiub Titanium Dioksida dalam Elektrolit Berasaskan Klorida:  
Suatu Alternatif kepada Elektrolit Berasaskan Flourida)

S.W. NG\*, F.K. YAM, K.P. BEH & Z. HASSAN

### ABSTRACT

*Often, fluoride based electrolyte was applied to synthesize highly ordered titanium dioxide nanotubes. However, in the present work, bundled titanium dioxide nanotubes were fabricated in chloride based electrolyte through electrochemical method. Structural and morphological investigations were carried out on the nanotubes synthesized under different anodization parameters. The growth mechanism of such nanotubes was elucidated and illustrated. The estimated diameter of the as-anodized nanotube was less than 150 nm while the length varied from hundreds of nanometer to microns. X-ray diffraction patterns and Raman spectra have showed anatase and rutile phases of titanium dioxide within the thermally treated samples.*

*Keywords: Anodization; chloride based electrolyte; growth mechanism; titanium dioxide nanotubes*

### ABSTRAK

*Kebiasaannya, elektrolit berasaskan flourida digunakan untuk menyediakan nanotiub titanium dioksida yang tersusun rapi. Namun begitu, dalam kertas ini, kelompok nanotiub titanium dioksida difabrikasi dalam elektrolit berdasarkan klorida melalui kaedah elektrokimia. Siasatan struktur dan morfologi dilakukan pada nanotiub yang disediakan dengan pelbagai parameter pengoksidaan. Mekanisme pertumbuhan nanotiub tersebut dijelas dan digambarkan. Diameter anggaran nanotiub yang disediakan adalah kurang daripada 150 nm manakala panjangnya berbeza daripada ratusan nanometer ke mikrometer. Corak pembelauan sinar X dan spektrum Raman menunjukkan fasa anatase dan rutil bagi titanium dioksida dalam sampel yang dirawat dengan terma.*

*Kata kunci: Elektrolit berasaskan klorida; mekanisme pertumbuhan; nanotiub titanium dioksida; pengoksidaan*

### INTRODUCTION

The investigation of titanium dioxide ( $\text{TiO}_2$ ), either in the form of thin film or nanostructures under various aspects has fascinated researchers for the past decades owing to its superior properties. Aside from its vast applications in chemical sensing, optoelectronics and storage medium,  $\text{TiO}_2$  is particularly well known for its water splitting capability which leads to the development of hydrogen based energy. Such innovation could possibly replace fossil fuels in near future, eventually solving the energy crisis of all mankind (Liu et al. 2009; Sang et al. 2012).

Among the various methods in obtaining  $\text{TiO}_2$  nanotubes, electrochemical process has always been favoured by most researchers as highly ordered arrays of such can be produced easily. Furthermore, extensive control over of the morphology of the nanotubes could be achieved by varying anodization parameters. In addition, the geometrical position of such nanotubes that erects perpendicular to the substrate is of importance, because this orientation provides an excellent pathway to transport electrical charges along their axial direction (Lamberti et al. 2013). Meanwhile, either bare titanium (Ti) itself, or substrates such as silicon wafer and indium-doped tin

oxide coated glass which is pre-sputtered with a Ti layer could be used as anode materials. For the anodization process, the commonly reported feature would be the use of fluoride based electrolyte. The essence of the fluorides could be derived from hydrofluoric acid, ammonium fluoride or sodium fluoride, which subsequently coupled with mixture of sodium sulphate, organic additives such as ethanol, ethylene glycol or glycerol, finally a tiny amount of acid to adjust the pH levels. Each of these components contributes in controlling the morphology and dimensions of the  $\text{TiO}_2$  nanotubes (Neupane et al. 2011; Shankar et al. 2006; Yoriya & Grimes 2011).

Despite the importance of fluoride ions in the formation of  $\text{TiO}_2$  nanotubes, could the latter be formed in the absence of the former? Several studies have reported the possibility of fabricating  $\text{TiO}_2$  nanotubes in chloride based electrolyte. The electrolyte employed by Richter et al. (2007a) consists of ammonium chloride, coupled with different types of acids, such as trichloroacetic, oxalic, gluconic, formic, sulphuric and hydrochloric (HCl). However, they drew a conclusion that these acids did not play a significant role in the formation of  $\text{TiO}_2$  nanotubes. Meanwhile, Allam and Grimes (2007) discovered that

the addition of low concentration phosphoric acid leads to the formation of nanorods rather than nanotubes. In accordance with Chen et al. (2007), in this work, we present a study of bundled  $\text{TiO}_2$  nanotubes fabricated through electrochemical method by using HCl as the main component in the electrolyte, which provides an acidic medium and concurrently supplies chloride source. Our study is relatively less reported as compared with the formation of highly ordered  $\text{TiO}_2$  nanotubes in fluoride based electrolyte. In addition, plausible formation mechanism and anodization parameters that affect the growth of  $\text{TiO}_2$  nanotubes are yet to be explored.

#### EXPERIMENTAL DETAILS

About 0.127 mm thick Ti foil (Strem Chemicals, 99.7%) was cut into pieces, then cleaned with sodium hydroxide solution, followed by ethanol and finally rinsed with deionized (DI) water. The anodization of Ti foil was carried out in a conventional two electrode electrochemical configuration with nickel as counter electrode. A constant potential of 10-30 V was applied for 1 h under room temperature ambient. The electrolyte consists of 1.0 M hydrogen peroxide ( $\text{H}_2\text{O}_2$ ), 1.0 M HCl and ethylene glycol (EG). The anodization conditions are listed in Table 1.

When the anodization process was completed, the samples were removed from the electrolyte, then rinsed with DI water, finally dried under air ambient. The morphology of the samples was observed by field emission scanning electron microscopy (FESEM, FEI Nova NanoSEM 450), while elemental compositions of the samples were determined by energy dispersive X-ray (EDX). The samples were subsequently heat treated in a tube furnace at 500°C for 1 h under air ambient for crystallization to occur. After that, the structural properties of the samples were determined by high resolution X-ray diffractometer (HR-XRD, PANalytical X'pert PRO MRD PW3040) with  $\text{CuK}\alpha_1$  source operating at 0.154 nm. Also, the vibrational properties of the thermal treated samples were studied using Raman spectroscopy (JobinYvon HR 800 UV) with 20 mW of  $\text{Ar}^+$  laser source at 514.5 nm. All measurements were performed under room temperature.

#### RESULTS AND DISCUSSION

The surface morphologies of all samples were depicted in Figure 1. For sample S1, random cracks with no appreciable structure were seen on the surface of Ti foil. When the applied potential was raised to 15 V (sample S2), definable tubular structure was found within the cracks and  $\text{TiO}_2$  nanotubes of less than 200 nm could be observed. When the applied potential was further increased to 20 and 30 V (sample S3 and S4, respectively), the nanotube diameter was extended and its length was elongated to more than 1  $\mu\text{m}$ . Based on these observations, it is therefore deduced that higher voltages would extend the nanotube lengths for anodization under the same reaction time. However, when sample S2 was further

anodized to 16 h (denoted as S5), the resultant nanotubes appeared to be a few microns long, with properly formed individual tube walls as shown in Figure 1(i) and 1(j).

When an applied potential was imposed on the system, the current instantaneously hiked to a maximum point. This is where the  $\text{Cl}^-$  ions from the electrolyte drifted towards Ti foil that acted as anode. The  $\text{Cl}^-$  ions randomly attacked the Ti foil to form pits and cracks. The cavities were scattered around the Ti surface but increase in terms of density when the applied potential was increased. This observation implies that a certain threshold voltage is required for the formation of bundled  $\text{TiO}_2$  nanotubes. Beneath the threshold voltage, only random cracks could be formed as noticed in Figure 1 (a) and 1(b).

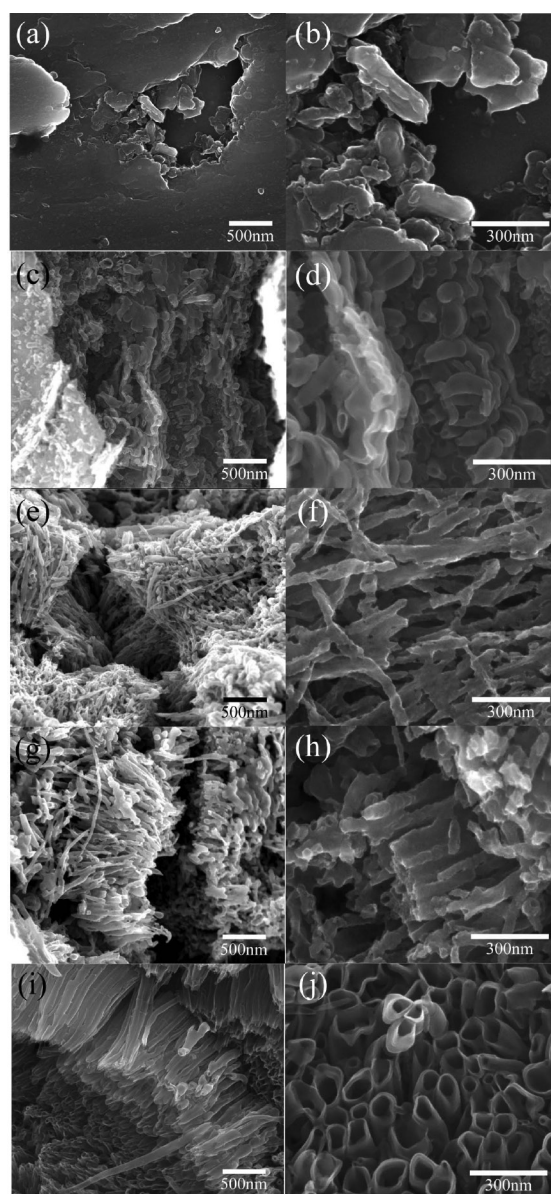
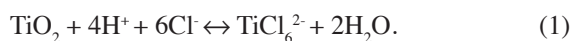


FIGURE 1. FESEM images show the surface morphology of the sample S1 (a, b), S2 (c, d), S3 (e, f), S4(g, h) and S5(i, j). Each sample was inspected at two different magnifications

After a short period, the current starts to decay and eventually reaches a steady state. During the decay of current, the electrolyte continues to supply  $\text{Cl}^-$  ions and these ions excavate the inner part of the cavity. When the current achieves a steady state, the formation of oxide layer begins and  $\text{TiO}_2$  nanotubes continue to elongate until the electrolyte ceases to supply  $\text{Cl}^-$  ions. The formation of  $\text{TiO}_2$  nanotubes under the influence of  $\text{Cl}^-$  is given in (1) which is analogous to that of  $\text{F}^-$  (Allam & Grimes 2007; Shankar et al. 2007).



For better understanding of the formation mechanism of  $\text{TiO}_2$  nanotubes in  $\text{Cl}^-$  ions electrolyte, the process is simplified in a schematic diagram in Figure 2.

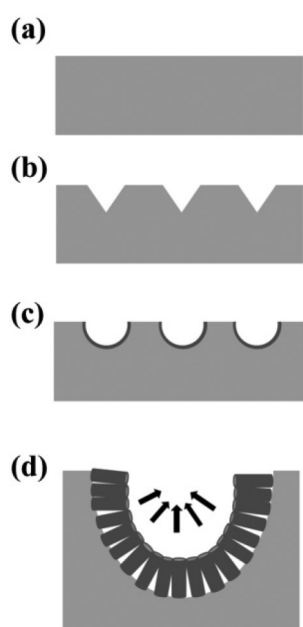


FIGURE 2. Schematic illustration of the formation of  $\text{TiO}_2$  nanotubes (a) Ti foil before potential was applied, (b) pits and cracks on the surface of Ti, (c) formation of oxide layer and (d) magnified view of one of the cavities, the growth direction of  $\text{TiO}_2$  nanotubes is oriented towards a common point

The increase in applied potential raises the electric field between the electrodes hence further accelerates the  $\text{Cl}^-$  ions towards the anode. Therefore, we noticed the increase of nanotube length corresponded with the rising anodization potential under constant duration as illustrated in Figure 1(c) and 1(h). However, prolonged anodization duration to 16 h nurtures the condition to form  $\text{TiO}_2$  nanotubes, as seen in Figure 1(i), the tubes wall was smoother and the tubes were arranged in a more orderly manner. In addition, we believed that the extension of nanotubes length was not linearly proportional to the anodization duration, based on the observation from Figure 1(c) and 1(i), the tubes length is estimated to be approximately 200 nm and 2  $\mu\text{m}$ , respectively. The oxide formation rate become lowered is ascribed to the reduced oxidation strength of  $\text{H}_2\text{O}_2$ .

For the anodization carried out in fluoride based electrolyte,  $\text{TiO}_2$  nanotubes are orthogonally erected on the surface of Ti and each tube is orderly connected to the adjacent neighbours to form a hierarchy (Shankar et al. 2007). In contrary, the  $\text{TiO}_2$  nanotubes formed in chloride based electrolyte orient to an invisible centric point of a cavity. It is conspicuous in Figure 1(i) that the nanotubes coincidentally point towards a same direction.

In addition, in this work, the variation of anodization potential did not give significant effects to the tube diameter which was in accordance with other investigations carried out in  $\text{Cl}^-$  ions electrolyte. Most reports claimed that the tube diameter was relatively small i.e. less than 50 nm (Chen et al. 2007; Rietcher et al. 2007b). However Figure 1(j) shows that the tube diameter could be up to 150 nm, which is comparable to that formed in  $\text{F}^-$  ions electrolyte.

During our preliminary studies, without EG addition, the attack of Ti surface by  $\text{Cl}^-$  ions is vigorous. Random areas on the Ti foil were over-etched; hence, tiny holes visible to naked eye were formed. We deduce that the rate of excavation on Ti foil was greater than the formation rate of the oxide layer; thus, EG was introduced in the electrolyte to decelerate the process. On the other hand,  $\text{H}_2\text{O}_2$  is a strong oxidizing agent which could increase the oxidation rate on Ti foil to produce a thicker oxide layer within a given period (Allam et al. 2008).

The qualitative analysis of the elements present in the as-anodized  $\text{TiO}_2$  nanotubes was evaluated by EDX and the results are composed in Table 2. It is apparent that Ti and

TABLE 1. Anodization conditions of all samples

Sample	Applied potential (V)	Duration (hr)	Temperature ( $^{\circ}\text{C}$ )	Composition of electrolyte (ratio)		
				$\text{H}_2\text{O}_2$	HCl	EG
S1	10	1	27	1	1	3
S2	15	1	27	1	1	3
S3	20	1	27	1	1	3
S4	30	1	27	1	1	3
S5	15	16	27	1	1	3

TABLE 2. Elemental composition of the selected as-anodized TiO<sub>2</sub> nanotubes

Elements	Atomic Percentage (%)	
	S2	S5
Titanium, Ti	46.12	28.62
Oxygen, O	52.54	56.23
Chlorine, Cl	1.34	2.76
Carbon, C	N/A	12.39
Total	100.00	100.00
Ratio O:Ti	1.14:1	1.96:1

O belong to TiO<sub>2</sub> nanotubes, while Cl and C originate from HCl and EG in the electrolyte. Sample S2 and S5 possess different O to Ti ratio, but the ratio of S5 is approximate to 2:1, corresponded to the stoichiometric ratio of TiO<sub>2</sub>.

Similar to the nanotubes fabricated in F<sup>-</sup> ions electrolyte, the as-anodized TiO<sub>2</sub> nanotubes are amorphous in nature (Allam & Grimes 2007; Neupane et al. 2011). Hence a simple thermal treatment was applied to transform the tubes to its crystalline phases. The XRD pattern of sample S5 is given in Figure 3.

Six Ti peaks were observed in the XRD patterns, correspond to (100), (002), (101), (102) (110) and (103) reflection, respectively. These peaks were originated from the Ti foil. Two anatase peaks positioned at 25.3 and 37.9° were separately indexed as (101) and (004) reflection, respectively. In addition, three rutile peaks located at 28.1, 36.1 and 56.4° were individually assigned to (110), (101) and (220) reflection, respectively (Neupane et al. 2011). These results suggested that TiO<sub>2</sub> nanotubes consist of a mixed crystalline phase of anatase and rutile.

TiO<sub>2</sub> in nature exhibits three types of crystalline phases i.e. anatase, rutile and brookite. In accordance with other reports, we observed only anatase and rutile phases in our samples. TiO<sub>2</sub> anatase phase possesses six active Raman modes A<sub>1g</sub> + 2B<sub>1g</sub> + 3E<sub>g</sub> whereas rutile crystalline structure has four active Raman modes A<sub>1g</sub> + B<sub>1g</sub> + B<sub>2g</sub> +

E<sub>g</sub> (Balachandran & Eror 1982). The Raman spectra of sample S2 and S5 were shown in Figure 4.

Both samples present a broad Raman band between 560-680 cm<sup>-1</sup> and the band could be resolved into two components, which were 612 and 638 cm<sup>-1</sup> that assigned to rutile A<sub>1g</sub> and anatase E<sub>g</sub>, respectively. Additionally, two anatase peaks were noticed at 395 and 515 cm<sup>-1</sup>, which were associated to anatase E<sub>g</sub> and A<sub>1g</sub> + B<sub>1g</sub>, respectively; while a rutile E<sub>g</sub> was found at 445 cm<sup>-1</sup> (Balachandran & Eror 1982). In brief, mixed modes of anatase and rutile were observed in both samples, with S2 being rutile dominant whereas S5 being anatase dominant.

We ascribe the discrepancy in peak intensities of both samples to the physical appearance of TiO<sub>2</sub> nanotubes. It is worth mentioning that longer anodization duration of sample S5 leads to greater tube length, hence thicker oxide layer. Studies have shown that the TiO<sub>2</sub> nanotubes are mainly anatase, whereas the barrier oxide layer between the nanotubes and Ti foil is comprised of rutile (Allam & Grimes 2007). Therefore, S5 with longer tubes is relatively rich in anatase grains.

#### CONCLUSION

TiO<sub>2</sub> nanotubes of a few microns long with diameter approximately 150 nm was fabricated by anodization process in chloride based electrolyte with H<sub>2</sub>O<sub>2</sub> and EG as additives. The formation mechanism was discovered to be partially similar to that of nanotubes fabricated in fluoride based electrolyte. The mechanism was discussed and illustrated in a schematic diagram. Although a certain threshold voltage is required to initiate the formation of nanotubes, overall tube diameter and length is independent to the applied potential. Prolonged anodization duration extends the tube length and produces smoother tube walls. The XRD results suggested that TiO<sub>2</sub> nanotubes consist of mixed anatase and rutile phases. The Raman results were well accorded to the XRD results, with both anatase

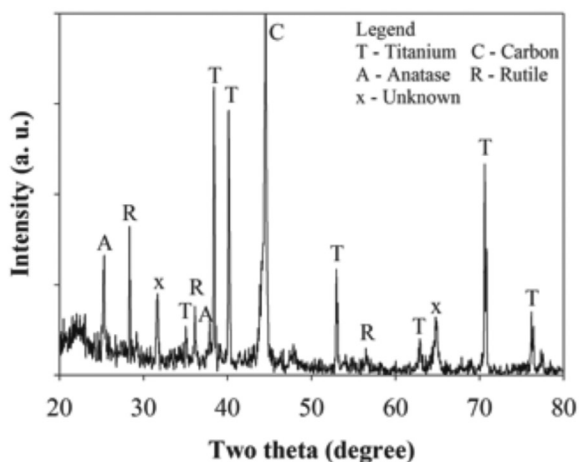


FIGURE 3. XRD pattern of sample S5 treated at 500°C for 1 h

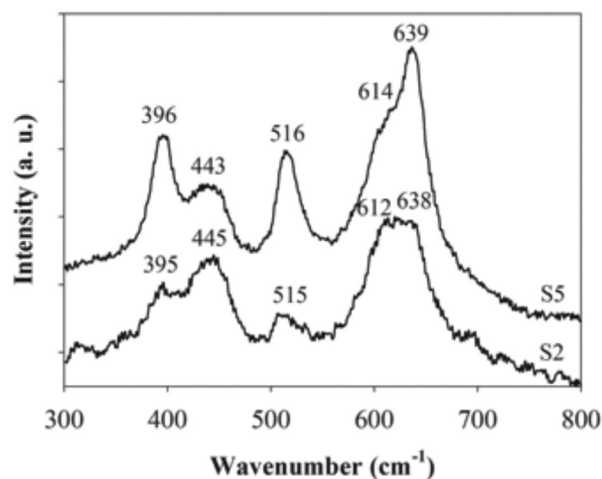


FIGURE 4. Raman spectra of sample S2 and S5

and rutile active modes were observed. The difference in peak intensities of the two different anodization duration samples was related to the tube length of the samples, whereby anatase was more prominent in the sample with thicker oxide layer. In general, the tube properties produced with Cl<sup>-</sup> ions are comparable to that of F<sup>-</sup> ions. Therefore, it can be served as an alternative electrolyte to produce TiO<sub>2</sub> nanotubes.

#### ACKNOWLEDGMENTS

This work was supported by USM ERGS 203/PFIZIK/6730096, RU-PRGS 1001/PFIZIK/834074 and 1001/PFIZIK/843087. The supports from Universiti Sains Malaysia is gratefully acknowledged.

#### REFERENCES

- Allam, N.K. & Grimes, C.A. 2007. Formation of vertically oriented TiO<sub>2</sub> nanotube arrays using a fluoride free HCl aqueous electrolyte. *Journal of Physical Chemistry C* 111: 13028-13032.
- Allam, N.K., Shankar, K. & Grimes, C.A. 2008. Photoelectrochemical and water photoelectrolysis properties of ordered TiO<sub>2</sub> nanotubes fabricated by Ti anodization in fluoride-free HCl electrolytes. *Journal of Materials Chemistry* 18: 2341-2348.
- Balachandran, U. & Eror, N.G. 1982. Raman spectra of titanium dioxide. *Journal of Solid State Chemistry* 42: 276-282.
- Chen, X., Schriver, M., Suen, T. & Mao, S.S. 2007. Fabrication of 10 nm diameter TiO<sub>2</sub> nanotube arrays by anodization. *Thin Solid Films* 515: 8511-8514.
- Lamberti, A., Sacco, A., Bianco, S., Manfredi, D., Cappelluti, F., Hernandez, S., Quaglio, M. & Pirri, C.F. 2013. Charge transport improvement employing TiO<sub>2</sub> nanotube arrays as front-side illuminated dye-sensitized solar cell photoanodes. *Physical Chemistry Chemical Physics* 15: 2596-2602.
- Liu, Z., Pesic, B., Raja, K.S., Rangaraju, R.R. & Misra, M. 2009. Hydrogen generation under sunlight by self-ordered TiO<sub>2</sub> nanotube arrays. *International Journal of Hydrogen Energy* 34: 3250-3257.
- Neupane, M.P., Park, I.S., Bae, T.S., Yi, H.K., Watari, F. & Lee, M.H. 2011. Synthesis and morphology of TiO<sub>2</sub> nanotubes by anodic oxidation using surfactant based fluorinated electrolyte. *Journal of the Electrochemical Society* 158: C242-C245.
- Richter, C., Panaitescu, E., Willey, R.J. & Menon, L. 2007a. Titania nanotubes prepared by anodization in fluorine-free acids. *Journal of Materials Research* 22: 1624-1631.
- Richter, C., Wu, Z., Panaitescu, E., Willey, R.J. & Menon, L. 2007b. Ultra-high-aspect-ratio titania nanotubes. *Advanced Materials* 19(7): 946-948.
- Sang, L.X., Zhang, Z.Y., Bai, G.M., Du, C.X. & Ma, C.F. 2012. A photoelectrochemical investigation of the hydrogen-evolving doped TiO<sub>2</sub> nanotube arrays electrode. *International Journal of Hydrogen Energy* 37: 854-859.
- Shankar, K., Mor, G.K., Prakasam, H.E., Yoriya, S., Paulose, M., Varghese, O.K. & Grimes, C.A. 2007. Highly-ordered TiO<sub>2</sub> nanotube arrays up to 220 μm in length: Use in water photoelectrolysis and dye-sensitized solar cells. *Nanotechnology* 18: 06570.
- Yoriya, S. & Grimes, C.A. 2011. Self-assembled anodic TiO<sub>2</sub> nanotube arrays: Electrolyte properties and their effect on resulting morphologies. *Journal of Materials Chemistry* 21: 102-108.

Nano-Optoelectronics Research and Technology Laboratory  
School of Physics, Universiti Sains Malaysia  
11800 Penang  
Malaysia

\*Corresponding author; email: sw.ng@live.com

Received: 29 March 2013

Accepted: 1 December 2013